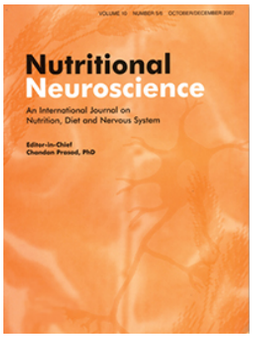

Taylor & Francis
Taylor & Francis Group

Nutritional Neuroscience

An International Journal on Nutrition, Diet and Nervous System

ISSN: 1028-415X (Print) 1476-8305 (Online) Journal homepage: http://www.tandfonline.com/loi/ynns20

Effect of catechins and high-temperature-processed green tea extract on scavenging reactive oxygen species and preventing $A\beta_{1-42}$ fibrils' formation in brain microvascular endothelium

Seon-Bong Lee, Eun-Hye Choi, Kang-Hyun Jeong, Kwang-Sik Kim, Soon-Mi Shim & Gun-Hee Kim

To cite this article: Seon-Bong Lee, Eun-Hye Choi, Kang-Hyun Jeong, Kwang-Sik Kim, Soon-Mi Shim & Gun-Hee Kim (2018): Effect of catechins and high-temperature-processed green tea extract on scavenging reactive oxygen species and preventing $A\beta_{1-42}$ fibrils' formation in brain microvascular endothelium, Nutritional Neuroscience, DOI: 10.1080/1028415X.2018.1507618

To link to this article: https://doi.org/10.1080/1028415X.2018.1507618

Published online: 15 Aug 2018.

Effect of catechins and high-temperature-processed green tea extract on scavenging reactive oxygen species and preventing $A\beta_{1-42}$ fibrils' formation in brain microvascular endothelium

Seon-Bong Lee[1†], Eun-Hye Choi [1†], Kang-Hyun Jeong[1], Kwang-Sik Kim[2], Soon-Mi Shim[1], Gun-Hee Kim[3]

[1]Department of Food Science and Biotechnology, Sejong University, 98 Gunja-dong, Gwangjin-gu, Seoul 143-747, Republic of Korea, [2]Pediatric Infectious Diseases, Johns Hopkins University, 600 N. Wolfe St, Park 256, Baltimore, MD 21287, USA, [3]Departments of Food and Nutrition, Duksung Women's University, Seoul 01369, Republic of Korea

The present study investigated the effect of high-temperature-processed green tea extract (HTP_GTE) and its bioactive components on the reduction of reactive oxygen species (ROS) and amyloid-beta (Aβ) protein in human microvascular endothelial cells. Compared to $A\beta_{1-42}$-only treatment, pretreatment of HTP_GTE was revealed to effectively inhibit ROS generation ($P<0.05$). HTP_GTE and catechins not only inhibit $A\beta_{1-42}$ fibril formation but also destabilize preformed $A\beta_{1-42}$ fibrils. The presence of HTP_GTE, $A\beta_{1-42}$ fibril formation was significantly inhibited in a dose-dependent manner at 12.5–100 μg/ml of HTP_GTE, showing 86–56%, respectively. Treatment of various concentrations of HTP_GTE and catechins steadily destabilized the preformed $A\beta_{1-42}$ fibrils for 24 h in a dose-dependent manner. It was observed that the gallated groups such as epigallocatechin gallate, epicatechin gallate, gallocatechin gallate, and catechin gallate more effectively disturbed $A\beta_{1-42}$ fibril formation and destabilized the preformed $A\beta_{1-42}$ fibrils than the non-gallated group. Taken together, these findings supported that sterilized green tea could be promising natural anti-amyloidogenic agents associated with therapeutic approaches in Alzheimer's disease by scavenging ROS generation and Aβ fibril in the brain tissue.

Keywords: High-temperature-processed green tea extract, Catechins, Reactive oxygen species, $A\beta_{1-42}$ fibrils, Blood-brain barrier

Introduction

Alzheimer's disease (AD) is an advanced neurodegenerative disease relating to most types of dementia.[1] By 2050, the number of AD patients is predictable to more than 106 million worldwide, and it is assessed that 1 in 85 persons will be existing with the AD.[2] Formation of amyloid-beta (Aβ) proteins as neuritic senile plaques' constituent is a key risk factor and it plays a central pathogenic role in the commencement and progression of AD.[3] The major species in Aβ proteins are the $A\beta_{1-40}$ and $A\beta_{1-42}$ peptides, with $A\beta_{1-42}$ being a hallmark of AD. $A\beta_{1-42}$ is considered more toxic than $A\beta_{1-40}$ as it could aggregate much more quickly than $A\beta_{1-40}$, leading to provide further Aβ-accumulation-related potential neurodegenerative disorders.[4,5]

A blood-brain barrier (BBB) located between the circulating blood and the brain not only forms an interface with tight junction but also retains various carrier-mediated transport systems.[6,7] The BBB also regulates transport of compounds by efflux transporters such as P-glycoprotein (P-gp) and multidrug-resistance-associated proteins in order to support and protect central nervous system.[8] Previous studies reported that Aβ induced numerous cytotoxic effects on neuronal cells and caused attenuation of the BBB through generation of reactive oxygen species (ROS).[9,10] ROS make functional changes of the BBB, leading to an increase in its permeability.[11,12] It is known to be a key component of the Aβ formation

†Co-first authors: Seon-Bong Lee and Eun-hye Choi contributed equally to the work.
Correspondence to: Soon-Mi Shim. Department of Food Science and Biotechnology, Sejong University, 98 Gunja-dong, Gwangjin-gu, Seoul 143-747, Republic of Korea. Email: soonmishim@sejong.ac.kr; Gun-Hee Kim Departments of Food and Nutrition, Duksung Women's University, Seoul 01369, Republic of Korea. Email: ghkim@duksung.ac.kr

DOI 10.1080/1028415X.2018.1507618

for neurodegeneration in AD.[13,14] Ujiie *et al.* (2003) also reported that structural changes to the BBB induced by increased Aβ could take a major role in AD progression.[15] Furthermore, Aβ accumulation in the synapse might be a damage to neuronal processes, which suggested that it could be a crucial factor that can affect the cognitive dysfunction of aged people and AD patients.[16,17]

The potential preventive action of phytochemicals has been recently focused on the neuronal death associated with neurodegenerative disorders. Several studies have demonstrated that polyphenols such as curcumin, resveratrol, and oligonol could inhibit Aβ-mediated damages.[18–20] Among them, green tea (*Camellia sinensis*), widely consumed around the world as well as contained catechins, was extensively studied due to its strong antioxidant activity.[21,22] For instance, it was well established that (–)-epigallocatechin gallate (EGCG) provided potential functions to protect neuronal cells from toxicity caused by Aβ.[23] Antioxidant compounds (–)-epicatechin (EC) and (+−)-catechin (C) also effectively attenuated Aβ generation.[24] Although other catechins presented in green tea have been known to provide free radical scavenging activity, it is limited to the anti-amyloidogenic activity of EGCG. Therefore, the present study aimed to evaluate the inhibitory activity against ROS induced by $A\beta_{1-42}$ and anti-amyloidogenic activity of catechins (epicatechins/non-epicatechins) and sterilized green tea extracts by using an *in vitro* BBB model system.

Materials and methods

Standards and chemical reagents

(–)-Epigallocatechin (EGC), (–)-EC, (–)-EGCG, (–)-epicatechin gallate (ECG), (–)-gallocatechin (GC), (–)-catechin (C), (–)-gallocatechin gallate (GCG), and (–)-catechin gallate (CG) standards were purchased from Wako (Osaka, Japan). High-temperature-processed green tea extract (HTP_GTE) was kindly provided by AmorePacific R&D Center (Gyeonggi-do, South Korea). Dulbecco's phosphate saline buffer (DPBS), Dulbecco's modified Eagle's medium (DMEM), and 0.25% trypsin EDTA and penicillin/streptomycin were purchased from Corning Costar (Corning, NY). Fetal bovine serum (FBS) was purchased from Biotechnics Research Inc. (Lake Forest, CA). $A\beta_{1-42}$ was purchased from Abcam (Cambridge, UK). The acetic acid solution was purchased from Sigma-Aldrich (St. Louis, MO, USA). Water and acetonitrile (HPLC grade) were purchased from J.T. Baker (Phillipsburg, NJ, USA).

Sample preparation

The stock of synthetic $A\beta_{1-42}$ was dissolved in 0.1% ammonia solution to yield a final concentration of 250 μM, separated into aliquots, and then stored at −80°C until use. For (3-(4,5-dimethylthiazol-2-yl)-2,5-diphenyltetrazolium bromide (MTT) assay and 2′, 7′-dichlorodihydrofluorescein diacetate (2′7′-DCFH-DA) assay, 25 μM of $A\beta_{1-42}$ was pre-incubated in DMEM without FBS for 24 h in order to form fibrils. Then, $A\beta_{1-42}$ was further diluted in a cell medium to obtain appropriate concentration. For the Thioflavin T (ThT) fluorescence assay, a stock solution of $A\beta_{1-42}$ was diluted to a concentration of 25 μM in phosphate buffer (50 mM, pH 7.5), containing 100 mM NaCl. Twenty five micrometer of $A\beta_{1-42}$ was used for further studies. Each catechin standards stock solutions was prepared in deionized distilled water. The stock solutions were stored at −80°C and diluted to the desired concentrations immediately before use.

Preparation of HTP_GTE

The *camellia sinensis* (CS) leaf used in this study was obtained from the Jeju-do in South Korea. The dried CS leaf (1000 g) was extracted two times with 50% aqueous ethanol (4 l × 3 times) using a heating bath at 60°C for 3 h to give 50% aqueous ethanol extract (255 g). The 50% aqueous ethanol extract was dissolved with 1l water and then subjected to a sterilization condition (at 121°C) for 90 minutes. The sterilized extract was concentrated with a rotary evaporator (Buchi R200) in vacuo (250 g).

Human brain microvascular endothelial cells cell culture

Human brain microvascular endothelial cells (HBMEC) were obtained from the Division of Pediatric Infectious Diseases, Johns Hopkins University School of Medicine (MD, USA).The cells were grown in DMEM supplement with 10% FBS and 1% penicillin/streptomycin. The cells were sustained in an incubator at 37°C with 5% CO_2 of atmosphere and 95% air. The growth medium was changed every other day.

Identification of bioactive components in HTP_GTE by UPLC-PDA-ESI-MS/MS

Bioactive components in HTP_GTE were determined by ultra-high performance liquid chromatography (UPLC) with a photodiode array (PDA) detector and electrospray ionization (ESI) mass spectrometry (MS). HTP_GTE were analyzed through a column chromatography with reversed phased-column (Shiseido, 250×4.6 mm, 5 μm, C18) with mobile phases of solvents A and B (A: 0.1% acetic acid in water, B: acetonitrile). The mobile phase gradient elution was accomplished by varying the ratio of solvents A and B with a 1 ml/min of flow rate. The injection volume was 20 μl. The initial phase of the gradient was 10% solvent B. Then, the gradient increased linearly to 15% of solvent B to 30 minutes, continuously

increased to 20% for the next 12 minutes, and held at 20% for 2 minutes. The gradient deceased to 10% of solvent B for 44.1 minutes and held at 10% to 50 minutes until analysis of the next sample. The UV wavelength was set at 280 nm. Mass spectra were carried out by using an LCQ fleet with ESI-MS. MS was achieved in a negative ion mode ($[M\text{-}H]^-$). ESI-MS conditions as follows: capillary voltage (−35.00 V), capillary temperature (270.00°C), source heater temperature (350.00°C), sheath gas flow (75.00), aux gas flow (40.00), tube lens (−70.00 V), source voltage (3.2 kV), and scan range (50–500 [m/z]).

Measurement of cell cytotoxicity

In accordance with the method reported in a previous study,[25,26] MTT assay was conducted to determine the inhibition of cell growth by 50% (IC_{50}). Briefly, HBMEC was seeded in the 96-well microplate at a density of 5×10^3 cells/well. After the HBMEC was attached to a 96-well microplate for 24 hours, the medium was removed, and then each well was washed by using DPBS. To determine the IC_{50} value of $A\beta_{1-42,}$ HBMEC was treated by various concentrations (1 nM, 10 nM, 100 nM, 1 μM, 10 μM, and 25 μM) of $A\beta_{1-42}$ for 24 hours. To confirm non-cytotoxic concentration ranges of HTP_GTE, treatments of HTP_GTE (12.5, 25, 50, 100, 200, 400, and 800 μg/ml) were added into cells and maintained for 24 hours. Concentrations of each treatment above 90% of cell viability were used for further study. Following treatment, the medium was removed and added to 100 μl of the MTT solution. Subsequently, 96-well microplate was incubated for 4 hours at 37°C under 5% of the CO_2 atmosphere. Cells were incubated after replacing the MTT solution with dimethyl sulfoxide. And then, using a microplate reader (Varioskan Flash, Thermo Scientific, San Jose, CA), optical density (O.D.) was measured at 570 nm. This operation was repeated in three times, and the average means were used in formula as follows:

$$\text{Percent of cell viability (\%)} = \frac{[\text{Average of test (O.D.)} - \text{Average of blank (O.D.)}]}{[\text{Average of control (O.D)} - \text{Average of blank (O.D)}]} \times 100$$

Measurement of intracellular ROS

In accordance with the method reported in previous studies,[25,27] 2′7′-DCFH-DA assay was carried out to measure intracellular ROS generation induced by $A\beta_{1-42.}$ Briefly, HBMEC was seeded in the 96-well black microplate at a density of 5×10^3 cells per well. After the cells were attached to a 96-well black microplate for 24 hours, the medium was removed, and then each well was washed by using DPBS. Subsequently, HBMEC was treated by various concentrations (1 nM, 10 nM, 100 nM, 1 μM, 10 μM, and 25 μM) of $A\beta_{1-42.}$ To determine ROS scavenging capacity of HTP_GTE, HBMEC was treated by various

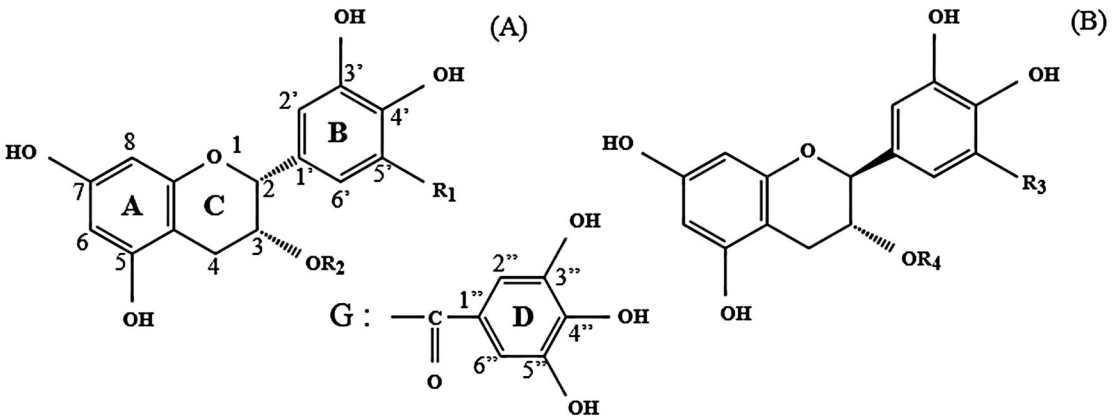

Components	R_1	R_2	R_3	R_4
(-)-Epigallocatechin (EGC)	OH	H	-	-
(-)-Epigallocatechin gallate (EGCG)	OH	G	-	-
(-)-Epicatechin (EC)	H	H	-	-
(-)-Epicatechin gallate (ECG)	H	G	-	-
(-)-Gallocatechin (GC)	-	-	OH	H
(-)-Gallocatechin gallate (GCG)	-	-	OH	G
(-)-Catechin (C)	-	-	H	H
(-)-Catechin gallate (CG)	-	-	H	G

Figure 1 Chemical structures of epicatechins (A) and non-epicatechins (B). * G: gallate

concentrations (12.5, 25, 50, and 100 μg/ml) of HTP_GTE for 2 hours and then, cells were treated with an IC_{50} value of $A\beta_{1-42}$ for 24 hours. After treatment, the medium was removed and 2′7′-DCFH-DA solution was added into each well followed by treating 0.25% trypsin EDTA. After reaction for 30 minutes at 37°C under 5% of the CO_2 atmosphere, the cell fluorescence was observed by using a microplate reader (Varioskan Flash, Thermo Scientific, San Jose, CA) at 488 nm for excitation and 525 nm for emission, respectively. This operation was repeated in three times, and the average means were used in formula as follows:

$$\text{Percent of ROS generation (\%)} = \left(\frac{\text{Average of test}}{\text{Average of control}}\right)\text{x}100$$

Measurement of $A\beta_{1-42}$ fibril formation and fibril destabilizing

Determination of fibril formation disrupts effect and fibril destabilizing effect was monitored by using a ThT binding assay. ThT specifically binds to the hydrophobic area on the surface of the β-sheet of $A\beta_{1-42}$, and thus the ThT fluorescence has been used as a quantitative indicator of amyloid fibrils,[28] and as a result, the dye exhibits red-shifted and enhanced fluorescence emission. To measure the inhibition effect of HTP_GTE and catechins on $A\beta_{1-42}$ fibril formation, 9 μl of 25 μM $A\beta_{1-42}$ was added to the 96-well black microplate, then incubated with 1 μl of each sample for 24 hours. Plates were covered to minimize evaporation without agitation. After incubation, 200 μl of ThT solution containing 50 mM glycine, NaOH buffer, pH 8.5, at a final concentration of 10 μM was added to each well. To measure the effect of fibril destabilizing by HTP_GTE and catechins, $A\beta_{1-42}$ was pre-incubated at 37°C for 24 hours to obtain $A\beta_{1-42}$ fibrils. After pre-incubation, 9 μl of 25 μM $A\beta_{1-42}$ was added to the black wells with 1 μl of each sample and incubated at various time intervals. Subsequently, 200 μl of ThT solution was added to each well and measured using a microplate reader (Varioskan Flash, Thermo Scientific, San Jose, CA) by fluorescence at 446 nm for excitation and 490 nm for emission, respectively. This operation was repeated in three times, and the average means were used in formula as follows:

$$\text{Relative fluorescence intensity(\%)} = \frac{[\text{Average of test (Fluorescence intesity)} - \text{Average of each sample blank(Fluorescence intesity)}]}{[\text{Average of control(Fluorescence intesity)} - \text{Average of each sample blank(Fluorescence intesity)}]} \times 100$$

Statistical analysis

Values were reported as the mean±standard deviation (SD) from at least three different experiments. Analysis of variance and Tukey's post hoc test were accomplished to determine significant differences among groups at the significance level of 0.05 by using Graphpad Prism 3.0 software (Graphpad, San Diego, CA).

Results

Identification of bioactive components in HTP_GTE by UPLC-PDA-ESI-MS/MS

As illustrated in Fig. 2A, eight major peaks from HTP_GTE were detected at 4.67, 7.18, 9.39, 15.97, 16.91, 19.92, 31.51, and 32.77 minutes of retention time, respectively by using UPLC-PDA. Structural identification of eight major bioactive components in HTP_GTE was detected in the negative ion mode with mass fragment patterns obtained by mass spectrometry (MS^1 and MS^2 spectra). Since epicatechins and non-epicatehins are structural isomers, EGC, EC, EGCG, and ECG showed same fragment patterns with their epimer, GC, C, GCG, and CG, respectively (Fig. 2B and 2C). In the mass spectra for the peak 1 and 2 ($[M\text{-}H]^-$) ion at m/z 305.06 was obtained from MS^1 and further fragmented to mainly m/z 261.08, 218.98, and 179.01 in MS^2. For the peak 3 and 4, ($[M\text{-}H]^-$) ion at m/z 289.06 produced ion at m/z 245.03, 205.09, and 179.06 on MS^2. In case of the peak 5 and 6, ($[M\text{-}H]^-$) ion at m/z 456.95 produced ion at m/z 331.02, 305.09, and 168.91 on MS^2. Peak 7 and 8 ($[M\text{-}H]^-$) ion at m/z 441.01 produced ion at m/z 331.00, 289.03, and 169.02 on MS^2. Epicatechins and non-epicatechins were determined by matching ions mass fragment patterns in both MS^1 and MS^2 spectra by comparing mass fragment patterns achieved from own standard. Hence, eight major components (including epicatechins and non-epicatechins) were used for further studies as individual bioactive components in HTP_GTE.

Cell cytotoxicity and ROS scavenging capacity of HTP_GTE induced by $A\beta_{1-42}$ in HBMEC

Figure 3 shows that HBMEC cell cytotoxicity by various concentrations of synthetic $A\beta_{1-42}$ was observed in a dose-dependent manner, showing 91, 89, 83, 77, 54, and 33% of cell viability ranged from 1 nM to 25 μM of $A\beta_{1-42,}$ respectively. Thus, the level of 10 μM $A\beta_{1-42}$ concentration was used for

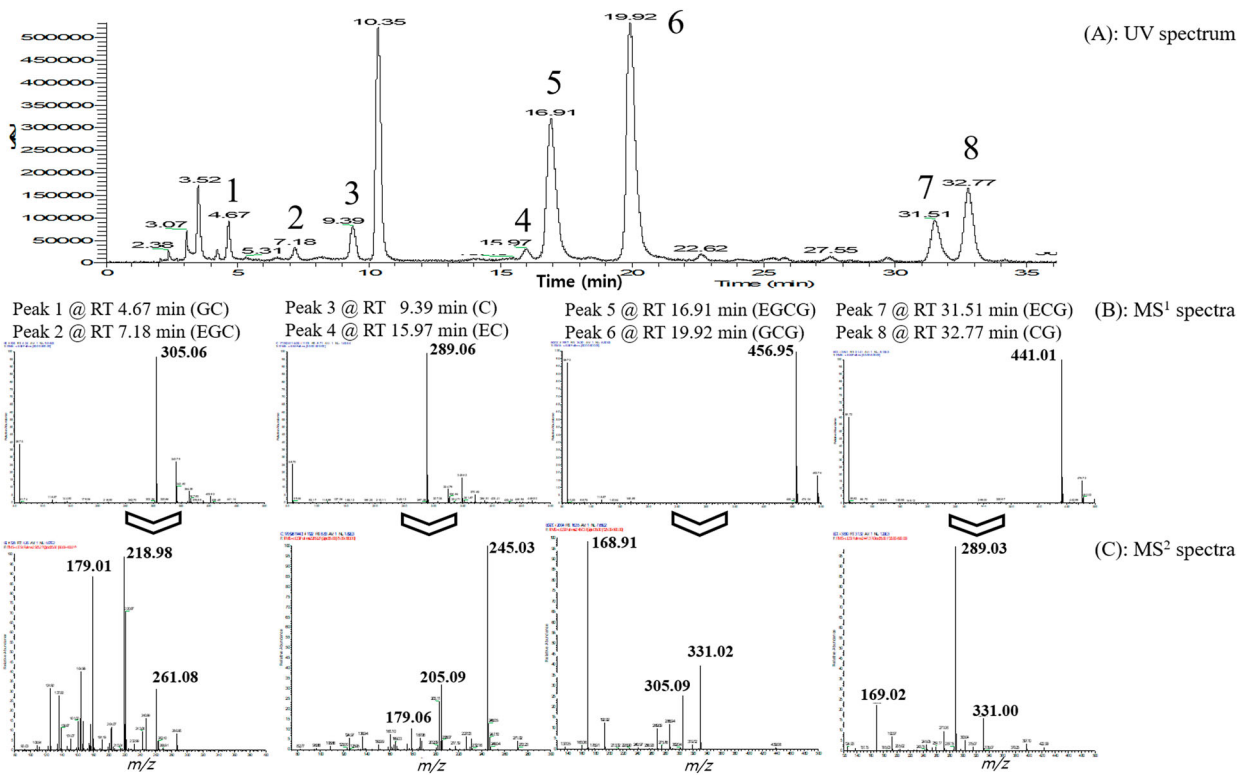

Figure 2 UPLC-UV spectrum and mass spectra of bioactive components in HTP_GTE

further study as IC_{50} value. ROS generation caused by $A\beta_{1–42}$ in HBMEC was also observed following exposure to 1 nM to 25 μM of $A\beta_{1–42}$ for 24 hours (Fig. 4A). This result indicates that $A\beta_{1–42}$ stimulated ROS generation resulting from cell apoptosis as reported in a previous study.[29] Hence, the protective effects of HTP_GTE on ROS generation induced by $A\beta_{1–42}$ were measured at various concentrations of HTP_GTE, 12.5, 25, 50, and 100 μg/ml, which were determined not to cause cell cytotoxicity (data not shown) to verify scavenging capacity of HTP_GTE (Fig. 4B). When HTP_GTE was pretreated, ROS generation was significantly attenuated, ranging from 105 to 107% compared to $A\beta_{1–42}$ only treatment ($P<0.05$). However, it was not shown in a dose-dependent manner. Particularly the most effective ROS scavenging ability was observed at 100 μg/ml concentration of HTP_GTE for protecting HBMEC against $A\beta_{1–42}$ exposure. These results suggest that HTP_GTE could modulate ROS induced by $A\beta_{1–42}$, the source of oxidative stress in terms of the cellular integrity of BBB, resulting in brain protection.

Inhibitory effects of HTP_GTE on $A\beta_{1–42}$ fibril formation and $A\beta_{1–42}$ fibril destabilization

The present study investigated the effects of HTP_GTE on $A\beta_{1–42}$ fibril formation using a ThT fluorescence assay. To measure the inhibitory

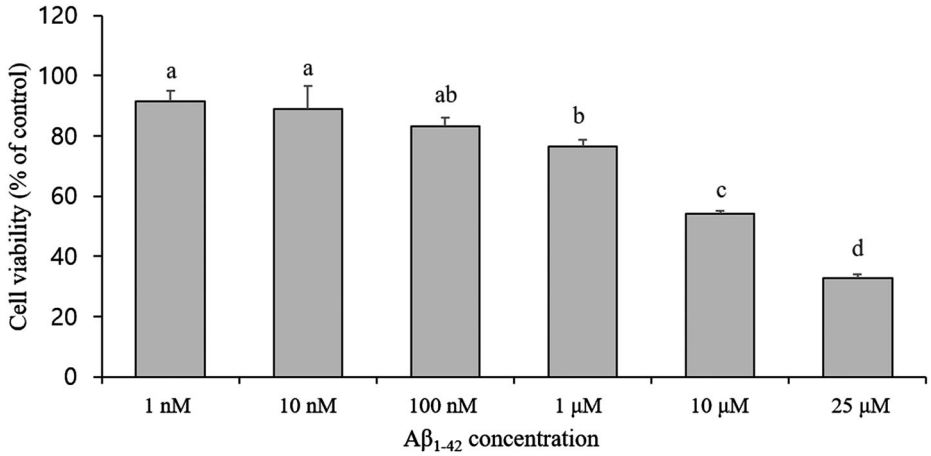

Figure 3 Cell viability (% of control) of HBMEC after $A\beta_{1–42}$ exposure for 24 h. Values are mean±SD of triplicate samples. Each bar with different letters is significantly different ($P<0.05$). Control indicates HBMEC treated by DMEM without $A\beta_{1–42}$

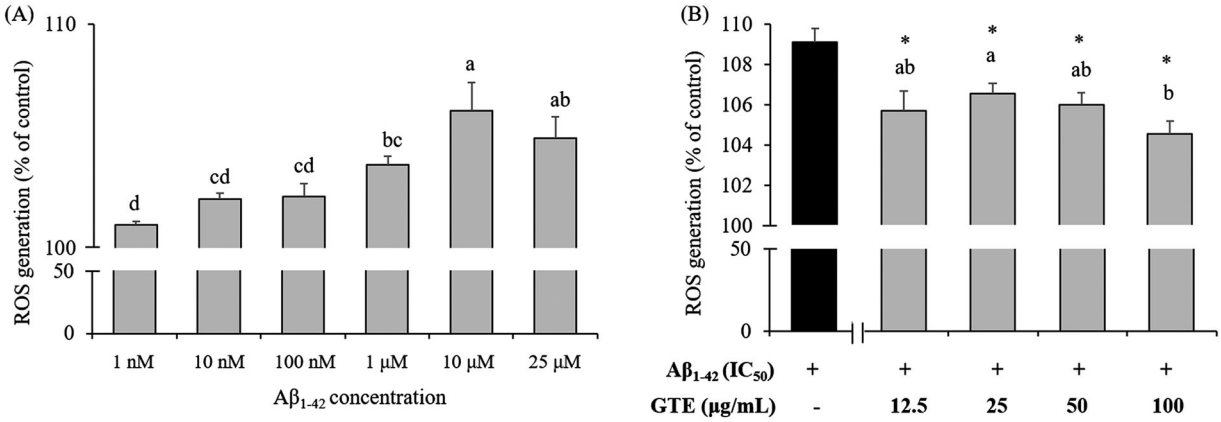

Figure 4 ROS generation (% of control) of HBMEC (A) and scavenging capacity of HTP_GTE on ROS (B) induced by $A\beta_{1-42}$ after incubating for 24 hours. Values are mean±SD of triplicate samples. Each bar with different letters is significantly different among treatments ($P<0.05$). * indicates a significant difference from $A\beta_{1-42}$ only treatment at $P<0.05$. Control indicates HBMEC treated by DMEM without $A\beta_{1-42}$

effects of HTP_GTE on $A\beta_{1-42}$ fibril formation, $A\beta_{1-42}$ was incubated for 24 hours at 37°C with various concentrations of HTP_GTE (12.5, 25, 50, 100 μg/ml) and then $A\beta_{1-42}$ fibril formation was expressed as relative fluorescence intensity (%). Figure 5A shows a fibril formation of $A\beta_{1-42}$ in

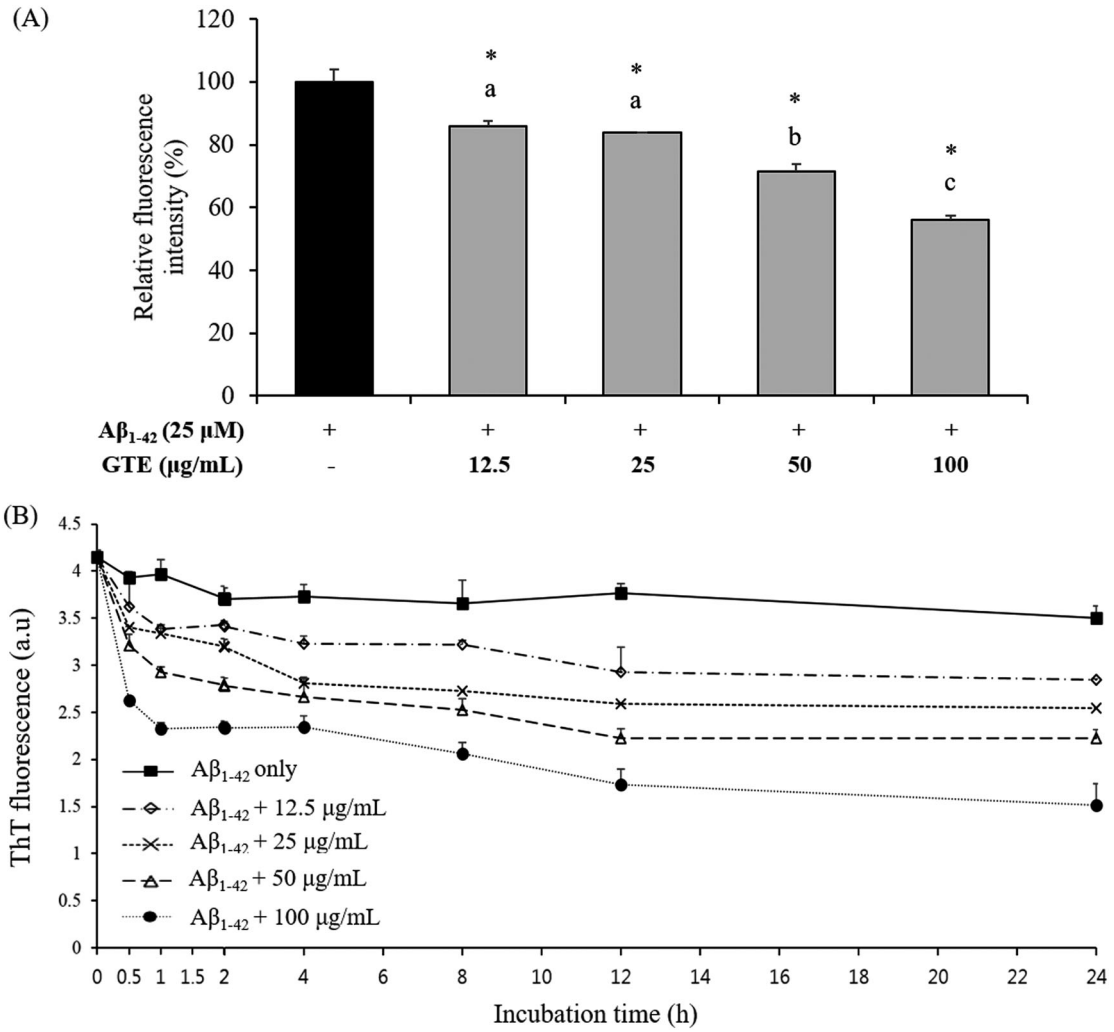

Figure 5 Inhibitory effects on $A\beta_{1-42}$ fibril formation after co-incubation with HTP_GTE for 24 hours (A) and effect of HTP_GTE on $A\beta_{1-42}$ fibril destabilization (B). For the destabilization effect, $A\beta_{1-42}$ was incubated at 37°C for 24 hours in 50 mM phosphate buffer prior to the experiment. The resulting $A\beta_{1-42}$ fibrils were then further incubated at 37°C with 12.5, 25, 50, and 100 μg/ml concentration of HTP_GTE. Values are mean±SD of triplicate samples ($n=3$). Each bar with different letters indicates a significant difference among treatments at $P<0.05$. * indicates a significant difference from $A\beta_{1-42}$ only treatment at $P<0.05$

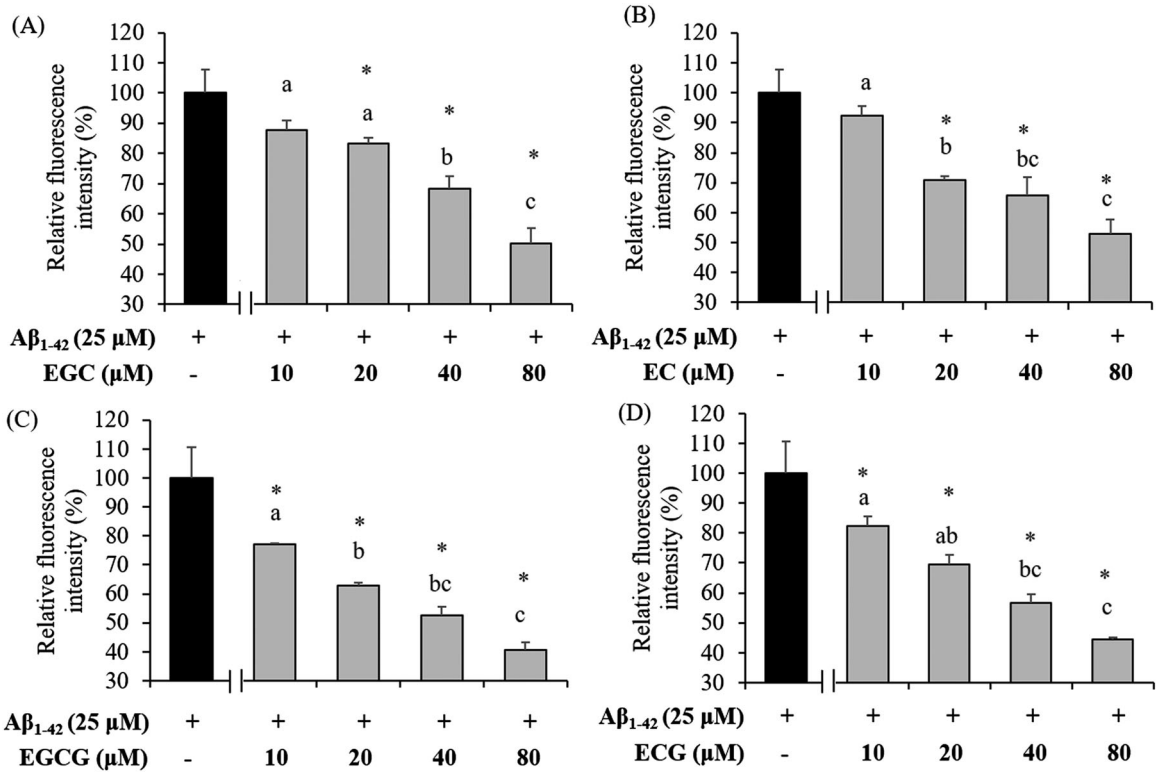

Figure 6 Inhibitory effects on $A\beta_{1-42}$ fibril formation after co-incubation with EGC (A), EC (B), EGCG (C), and ECG (D) for 24 hours. Values are mean±SD of triplicate samples. Each bar with different letters indicates a significant difference among treatments at $P<0.05$. * indicates a significant difference from $A\beta_{1-42}$ only treatment at $P<0.05$

the presence or absence of HTP_GTE. The presence of HTP_GTE, $A\beta_{1-42}$ fibril formation was significantly inhibited in a dose-dependent manner at 12.5–100 μg/ml of HTP_GTE, showing 86–56%, respectively. It indicates that 100 μg/ml of HTP_GTE could obviously inhibit $A\beta_{1-42}$ fibril formation. However, there was no significant difference between 12.5 and 25 μg/ml of HTP_GTE ($P>0.05$). One of the existing therapeutic approaches in the AD is to destabilize preformed fibrils in order to make Aβ clearance. Therefore, we further investigated the fibril destabilizing effects of HTP_GTE (Fig. 5B). ThT fluorescence was almost unchanged and showed the highest levels during the incubation of fresh $A\beta_{1-42}$ at 37°C without HTP_GTE. After adding various concentrations of HTP_GTE, ThT fluorescence was considerably decreased between 0 and 1 hour of incubation time in all treatments and steadily decreased for 24 hours in a dose-dependent manner. Especially, the addition of 100 μg/ml HTP_GTE inhibition showed the highest activity to destabilize preformed fibrils during 24 hours of incubation. These results indicated that HTP_GTE could significantly inhibit and destabilize amyloid oligomer formation associated with AD due to catechins in HTP_GTE. Hence, we further studied the effects of bioactive components in HTP_GTE on an anti-$A\beta_{1-42}$ activity in detail.

Inhibitory effects of epicatechins and non-epicatechins on $A\beta_{1-42}$ fibril formation

To measure the inhibitory effects of epicatechins (EGC, EC, EGCG, and ECG) on $A\beta_{1-42}$ fibril formation, $A\beta_{1-42}$ was incubated for 24 hours at 37°C with various concentrations of epicatechins (10, 20, 40, and 80 μM) and $A\beta_{1-42}$ fibril formation was expressed as relative fluorescence intensity (%) (Fig. 6). In all groups, relative fluorescence intensity as a surrogate of $A\beta_{1-42}$ fibril formation was attenuated by epicatechins in a dose-dependent manner at all the concentrations. EGC inhibited relative fluorescence intensity at all the concentrations in a dose-dependent manner, ranged from 88 to 50% for 10–80 μM of concentrations, respectively (Fig. 6A). Relative fluorescence intensity by pretreatment of EC ranged from 92 to 53%, indicating a pattern with EGC (Fig. 6B). However, in contrast to EGC, a dramatic decreasing was observed between 10 and 20 μM of EC, showing 92–71%, respectively. Although each relative fluorescence intensity decreased by 88 or 92% at 10 μM concentration of EGC or EC, there was no significant difference between $A\beta_{1-42}$ treatment only and 10 μM of EGC or EC treatment ($P>0.05$), respectively. It was also observed that the gallated groups such as EGCG and ECG disturbed $A\beta_{1-42}$ fibril formation, indicating that relative fluorescence intensity was ranging from

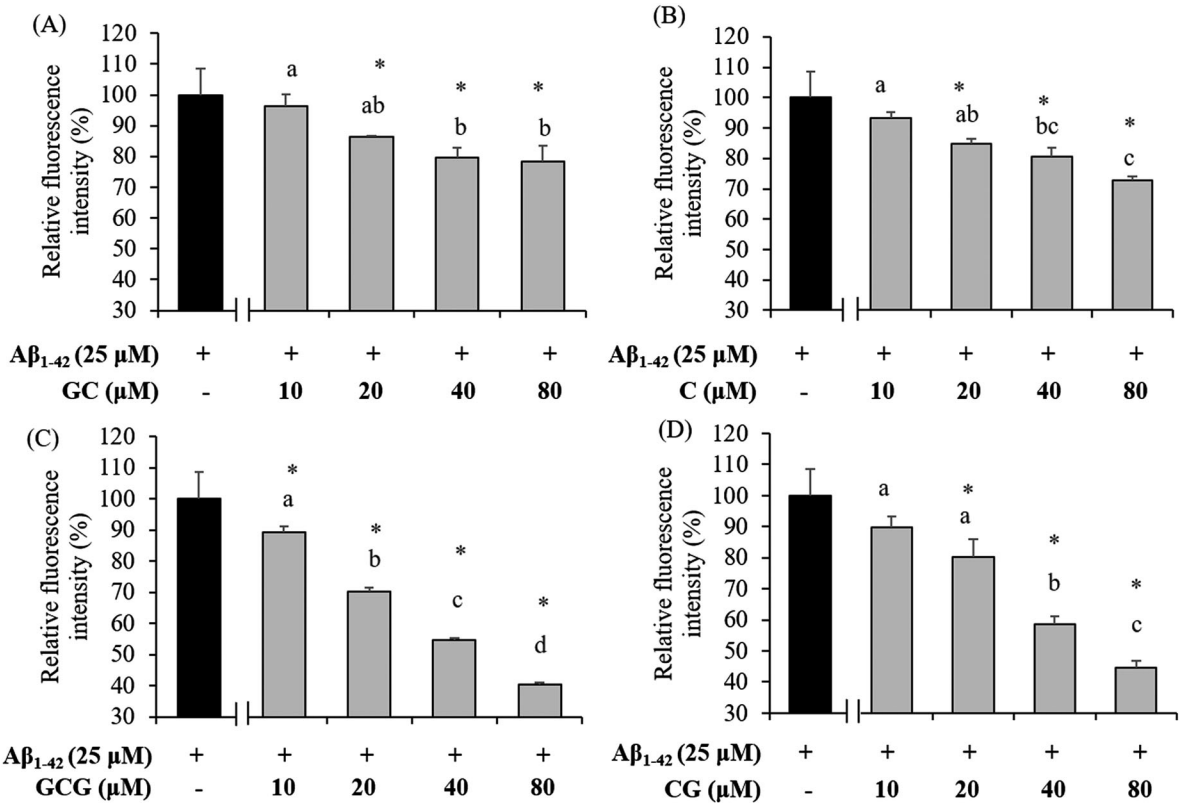

Figure 7 Inhibitory effects on $A\beta_{1-42}$ fibril formation after co-incubation with GC (A), C (B), GCG (C), and CG (D) for 24 hours. Values are mean±SD of triplicate samples. Each bar with different letters indicates a significant difference among treatments at $P<0.05$. * indicates a significant difference from $A\beta_{1-42}$ only treatment at $P<0.05$

77 to 41% and from 82 to 44% for 10–80 μM of EGCG (Fig. 6C) and ECG (Fig. 6D), respectively. Both EGCG and ECG showed the linear decreasing pattern on $A\beta_{1-42}$ fibril formation; especially EGCG showed a higher inhibition effect on $A\beta_{1-42}$ fibril formation than that of ECG. Our results suggest that epicatechins could effectively disrupt $A\beta_{1-42}$ fibril formation associated with the AD. Since non-epicatechins are other components in green tea, we performed further experiments for measuring the inhibitory effects of non-epicatechins on $A\beta_{1-42}$ fibril formation (Fig. 7). In all groups, relative fluorescence intensity was attenuated by non-epicatechins in a dose-dependent manner at all the concentrations (10, 20, 40, and 80 μM), implying that epicatechins as well as non-epicatechins in green tea inhibited $A\beta_{1-42}$ fibril formation. In detail, the relative fluorescence intensity in a GC and C treatment ranged from 96 to 78% and 93 to 73%, respectively (Fig. 7A and 7B). The gallated groups such as GCG and CG remarkably disturbed $A\beta_{1-42}$ fibril formation, showing 89–40% and 90–45% of relative fluorescence intensity for GCG (Fig. 7C) and CG (Fig. 7D), respectively. Apart from other groups, all the values in the GCG group showed a significant difference when compared to $A\beta_{1-42}$-only treatment ($P<0.05$). Compared to other non-epicatechins, the level of $A\beta_{1-42}$ fibril formation treated with GCG showed the lowest at all concentrations, indicating that GCG provided relatively higher inhibition activity than others.

Effects of epicatechins and non-epicatechins on $A\beta_{1-42}$ fibril destabilization

The destabilizing effect of catechins on $A\beta_{1-42}$ fibril was evaluated during 24 hours incubation with the presence of 80 μM of each catechin at 37°C and it was expressed as % of aggregation (Fig. 8). In all groups, marked destabilizing was observed between 0 and 0.5 hours of incubation time. The efficiency of destabilizing $A\beta_{1-42}$ fibril was in the order of EGCG > GCG > CG > ECG > GC > EGC > EC > C. Gallated groups such as EGCG, ECG, GCG, and CG showed a much higher destabilizing effect compared to non-gallated groups. Especially, it was shown that EGCG has the highest ability in disaggregation of $A\beta_{1-42}$ fibril by showing 44% at 24 hours followed by GCG. In the case of non-gallated catechins, GC showed the highest destabilizing effect on $A\beta_{1-42}$ fibril among non-gallated catechins, having 81% at 24 hours of incubation time. These results implied that green tea catechins could protect the brain against an AD by destabilizing effect on $A\beta_{1-42}$ fibril.

Discussion

Here, we demonstrated that the HTP_GTE and its bioactive components, catechins (including

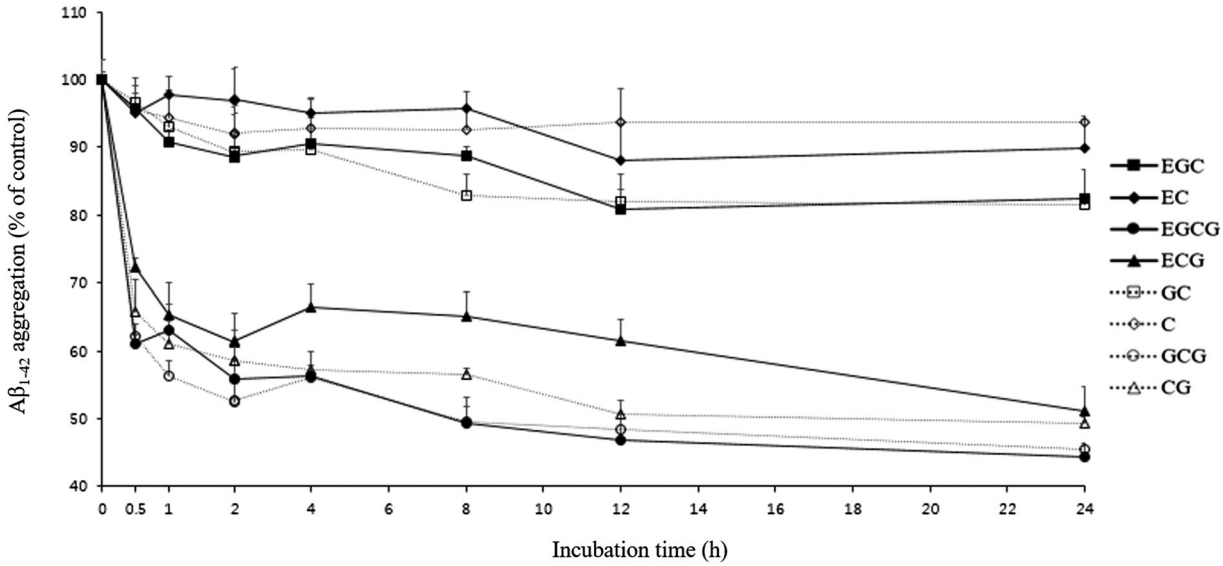

Figure 8 Effects on $A\beta_{1-42}$ fibril destabilization by epicatechins and non-epicatechins. $A\beta_{1-42}$ was incubated at 37℃ for 24 hours in 50 mM phosphate buffer prior to the experiment. The resulting $A\beta_{1-42}$ fibrils were then further incubated at 37℃ with 80 μM of each catechin. Values are mean±SD of triplicate samples (n=3).

epicatechins and non-epicatechins), exhibited ROS scavenging capacity in HBMEC induced by $A\beta_{1-42}$ as well as anti-amyloidogenic effects such as fibril formation and fibril destabilization *in vitro*. Misonou *et al.* (2000) reported that oxidative stress induced by hydrogen peroxide (H_2O_2) increased the intracellular Aβ levels in human neuroblastoma SH-SY5Y cells.[30] Other previous studies also found that oxidative stress induced by Aβ peptides directly initiate ROS formation associated with cellular dysfunction, mitochondrial dysfunction, and neuronal death in the pathogenesis of AD.[31,32] Based upon results from the present study, Aβ could induce ROS generation in the human brain endothelial cell line (Fig. 4A). It could be considered that Aβ and ROS are in a close relationship with each other in neuronal disorder, leading to the AD. Thus, plant extracts containing the flavonoids have been extensively studied for modulation of oxidative status induced by Aβ. For instance, Bastianetto *et al.*, 2000 investigated the antioxidant capacity of *Ginkgo biloba* extract obtained from green leaves against the intracellular and mitochondrial ROS in rat hippocampal cells induced by Aβ peptides.[33] Like our results, intracellular and mitochondrial ROS levels were reduced 85, 65, 49%, and 88, 75, 64%, respectively, at 10, 50, and 100 μg/ml concentrations of *Ginkgo biloba* extract after exposure to cells. According to the previous study, *Ginkgo biloba* leaves contained 167 μg/g of EC, the most abundant compound among other flavonoids, followed by rutin (135 μg/g), apigenin (32.6 μg/g), quercetin (11.0 μg/g), and luteolin (10.4 μg/g).[34] In addition, it was demonstrated that HTP_GTE treatment substantially reduced oxidative DNA damage by reducing the formation of 8-hydroxydeoxyguanosine, which has been implicated in neuronal cell death by $A\beta_{25-35}$.[35,36] Hence, these findings support our result that HTP_GTE could effectively contribute to prevention of AD by restraining of Aβ accumulation induced by oxidative stress through the antioxidant activity.

A previous study established that $A\beta_{1-42}$ peptides contain two stacked parallel β-sheet structure.[37] The formation of ordered β-sheet structures is predominantly a consequence of the formation of highly directional inter-chain hydrogen bonds.[38] Therefore, the structure activity relationships of polyphenols have been considered for a steric interference in β-sheet interaction, resulting in not only inhibition but also destabilization of Aβ. Several other known inhibitors supporting this fact, OH substitutors, blocked Aβ aggregation by hydrogen bonding with β-sheet of Aβ.[39,40] The number of hydroxyl groups on each side of the molecule is related to the anti-amyloidogenic activity of polyphenol. The more OH groups in the molecular structure, the higher the anti-amyloidogenic activity was shown.[41] Previous studies suggested that EGCG could act as anti-amyloidogenic agents by both binding to the Aβ structure and modifying the pathway to form non-toxic oligomers and stabilizes amyloidogenic proteins, preventing them from forming the amorphous aggregates associated with fibril formation.[42,43] Since EGC, EC, EGCG, and ECG have 6, 5, 8, and 7 of OH groups as shown in Fig. 1, these aspects support our results that gallated groups showed higher anti-amyloidogenic activity than non-gallated groups on inhibition of $A\beta_{1-42}$ fibril formation and fibril destabilizing of $A\beta_{1-42}$ peptides (Figs. 6 and 8). GC, C, GCG, and CG have the same

number of OH groups with each EGC, EC, EGCG, and ECG, respectively; thus non-epicatechins also showed similar patterns with the results of epicatehins (Figs. 7 and 8). Furthermore, the number of OH groups is associated with not only anti-amyloidogenic activity but antioxidant activity. It was established that the antioxidant activity related to the chemical structure was found to be reliable on the number of OH or NH_2 groups.[44] This result means that both antioxidant activity and anti-amyloidogenic activity are closely related. In addition, Ono *et al*. (2003) reported that chirality of catechins is another factor affecting the anti-amyloidogenic.[39] Epicatehins and non-epicatechins have a chirality to each other, thus this difference in the three-dimensional structure of polyphenols would greatly affect the anti-amyloidogenic activity. Therefore, it may be reasonable to consider that polyphenols with antioxidant motifs could bind specifically to Aβ, inhibiting Aβ formation or destabilizing preformed Aβ. To our knowledge, there is limited information on the inhibitory effects of whole catechins, bioactive components in HTP_GTE on $A\beta_{1-42}$ as a hall mark of the AD.

In conclusion, the present study demonstrated that sterilized green tea was able to attenuate the generation of ROS in human brain endothelial cell line and provide a potent anti-amyloidogenic activity in an *in vitro* system. HTP_GTE effectively contribute to oxygen radicals' scavenging ability induced by $A\beta_{1-42}$. HTP_GTE and their bioactive components also destabilized of $A\beta_{1-42}$ as well as inhibited $A\beta_{1-42}$ fibril formation, which is known to be a crucial pathological factor of the AD. Taken together, these findings supported that sterilized green tea could be an efficient natural product to reduce ROS generation in the brain tissue and enhance clearance of Aβ associated with therapeutic approaches in the AD.

Acknowledgment

This research was part of a projected titled "Development of Global Senior-friendly Health Functional Food Materials from Marin Resources" funded by the Ministry of Oceans and Fisheries, Korea. Also, this work was supported in part by the US National Institutes of Health (NIH) grant, NS091102 to KSK.

Disclaimer statement

Contributor None.

Conflicts of interest The authors have declared no conflict of interest.

Ethics approval None.

ORCID

Eun-Hye Choi http://orcid.org/0000-0002-6849-3222

References

1 Filley C. Alzheimer's disease: it's irreversible but not untreatable. Geriatrics 1995;50(7):18–23.
2 Brookmeyer R, Johnson E, Ziegler-Graham K, Arrighi HM. Forecasting the global burden of Alzheimer's disease. Alzheimers Dement 2007;3(3):186–91.
3 Findeis MA. The role of amyloid β peptide 42 in Alzheimer's disease. Pharmacol Ther 2007;116(2):266–86.
4 Burdick D, Soreghan B, Kwon M, Kosmoski J, Knauer M, Henschen A, et al. Assembly and aggregation properties of synthetic Alzheimer's A4/beta amyloid peptide analogs. J Biol Chem 1992;267(1):546–54.
5 Haass C, Hung AY, Selkoe DJ, Teplow DB. Mutations associated with a locus for familial Alzheimer's disease result in alternative processing of amyloid beta-protein precursor. J Biol Chem 1994;269(26):17741–8.
6 Ohtsuki S, Terasaki T. Contribution of carrier-mediated transport systems to the blood–brain barrier as a supporting and protecting interface for the brain; importance for CNS drug discovery and development. Pharm Res 2007;24(9):1745–58.
7 Ronaldson PT, Davis PT. Blood-brain barrier integrity and glial support: mechanisms that can be targeted for novel therapeutic approaches in stroke. Curr Pharm Des 2012;18(25):3624–44.
8 Golden PL, Pollack GM. Blood–brain barrier efflux transport. J Pharm Sci 2003;92(9):1739–53.
9 Carrano A, Hoozemans JJ, van der Vies SM, Rozemuller AJ, van Horssen J, de Vries HE. Amyloid beta induces oxidative stress-mediated blood–brain barrier changes in capillary amyloid angiopathy. Antioxid Redox Signal 2011;15(5):1167–78.
10 Tsoy A, Shalakhmetova T, Umbayev B, Askarova S. Role of ROS in Aβ42 mediated cell surface P-selectin expression and actin polymerization. Neurol Asia 2014;19(3).
11 Schreibelt G, Musters RJ, Reijerkerk A, de Groot LR, van der Pol SM, Hendrikx EM, et al. Lipoic acid affects cellular migration into the central nervous system and stabilizes blood-brain barrier integrity. J Immunol 2006;177(4):2630–37.
12 Haorah J, Ramirez SH, Schall K, Smith D, Pandya R, Persidsky Y. Oxidative stress activates protein tyrosine kinase and matrix metalloproteinases leading to blood–brain barrier dysfunction. J Neurochem 2007;101(2):566–76.
13 Butterfield DA, Lauderback CM. Lipid peroxidation and protein oxidation in Alzheimer's disease brain: potential causes and consequences involving amyloid β-peptide-associated free radical oxidative stress 1, 2. Free Radic Biol Med 2002;32(11):1050–60.
14 Varadarajan S, Yatin S, Aksenova M, Butterfield DA. Alzheimer's amyloid β-peptide-associated free radical oxidative stress and neurotoxicity. J Struct Biol 2000;130(2–3):184–208.
15 Ujiie M, Dickstein DL, Carlow DA, Jefferies WA. Blood–brain barrier permeability precedes senile plaque formation in an Alzheimer disease model. Microcirculation 2003;10(6):463–70.
16 Walsh DM, Klyubin I, Fadeeva JV, Cullen WK, Anwyl R, Wolfe MS, et al. Naturally secreted oligomers of amyloid β protein potently inhibit hippocampal long-term potentiation in vivo. Nature 2002;416(6880):535–39.
17 Hsia AY, Masliah E, McConlogue L, Yu GQ, Tatsuno G, Hu K, et al. Plaque-independent disruption of neural circuits in Alzheimer's disease mouse models. Proc Natl Acad Sci 1999;96(6):3228–33.
18 LI MH, JANG JH, Sun B, SURH YJ. Protective effects of oligomers of grape seed polyphenols against β-amyloid-induced oxidative cell death. Ann N Y Acad Sci 2004;1030(1):317–29.
19 Lim GP, Chu T, Yang F, Beech W, Frautschy SA, Cole GM. The curry spice curcumin reduces oxidative damage and amyloid pathology in an Alzheimer transgenic mouse. J Neurosci 2001;21(21):8370–7.
20 Thapa A, Jett SD, Chi EY. Curcumin attenuates amyloid-β aggregate toxicity and modulates amyloid-β aggregation pathway. ACS Chem Neurosci 2015;7(1):56–68.
21 Henning SM, Niu Y, Lee NH, Thames GD, Minutti RR, Wang H, et al. Bioavailability and antioxidant activity of tea flavanols after consumption of green tea, black tea, or a green tea extract supplement. Am J Clin Nutr 2004;80(6):1558–64.
22 Kondo K, Kurihara M, Miyata N, Suzuki T, Toyoda M. Scavenging mechanisms of (-)-epigallocatechin gallate and (-)-epicatechin gallate on peroxyl radicals and formation of superoxide during the inhibitory action. Free Radic Biol Med 1999;27(7):855–63.

23 Levites Y, Amit T, Mandel S, Youdim MB. Neuroprotection and neurorescue against Aβ toxicity and PKC-dependent release of nonamyloidogenic soluble precursor protein by green tea polyphenol (-)-epigallocatechin-3-gallate. FASEB J 2003;17(8):952–54.
24 Ono K, Yamada M. Antioxidant compounds have potent anti-fibrillogenic and fibril-destabilizing effects for α-synuclein fibrils in vitro. J Neurochem 2006;97(1):105–15.
25 Seo SB, Choe ES, Kim KS, Shim SM. The effect of tobacco smoke exposure on the generation of reactive oxygen species and cellular membrane damage using co-culture model of blood brain barrier with astrocytes. Toxicol Ind Health 2017;33(6):530–36.
26 Kim YM, Jeon YJ, Huh JS, Kim SD, Park KK, Cho M. Effects of enzymatic hydrolysate from seahorse hippocampus abdominalis on testosterone secretion from TM3 Leydig cells and in male mice. Appl Biol Chem 2016;59(6):869–79.
27 Kwon YK, Choi SJ, Kim CR, Kim JK, Kim YJ, Choi JH, et al. Antioxidant and cognitive-enhancing activities of Arctium lappa. Appl Biol Chem 2016;59(4):553–65.
28 Levine H. Thioflavine T interaction with synthetic Alzheimer's disease β-amyloid peptides: detection of amyloid aggregation in solution. Protein Sci 1993;2(3):404–10.
29 Liu L, Gu L, Ma Q, Zhu D, Huang X. Resveratrol attenuates hydrogen peroxide-induced apoptosis in human umbilical vein endothelial cells. Eur Rev Med Pharmacol Sci 2013;17(1):88–94.
30 Misonou H, Morishima-Kawashima M, Ihara Y. Oxidative stress induces intracellular accumulation of amyloid β-protein (Aβ) in human neuroblastoma cells. Biochem 2000;39(23):6951–9.
31 Shelat PB, Chalimoniuk M, Wang JH, Strosznajder JB, Lee JC, Sun AY, et al. Amyloid beta peptide and NMDA induce ROS from NADPH oxidase and AA release from cytosolic phospholipase A2 in cortical neurons. J Neurochem 2008;106(1):45–55.
32 Manczak M, Anekonda TS, Henson E, Park BS, Quinn J, Reddy PH. Mitochondria are a direct site of Aβ accumulation in Alzheimer's disease neurons: implications for free radical generation and oxidative damage in disease progression. Hum Mol Genet 2006;15(9):1437–49.
33 Bastianetto S, Ramassamy C, Doré S, Christen Y, Poirier J, Quirion R. The ginkgo biloba extract (EGb 761) protects hippocampal neurons against cell death induced by β-amyloid. Eur J Neurosci 2000;12(6):1882–90.
34 Cao Y, Chu Q, Fang Y, Ye J. Analysis of flavonoids in Ginkgo biloba L. and its phytopharmaceuticals by capillary electrophoresis with electrochemical detection. Anal Bioanal Chem 2002;374(2):294–9.
35 Hong JT, Ryu SR, Kim HJ, Lee JK, Lee SH, Yun YP, et al. Protective effect of green tea extract on ischemia/reperfusion-induced brain injury in Mongolian gerbils. Brain Res 2001;888(1):11–18.
36 Hong JT, Ryu SR, Kim HJ, Lee JK, Lee SH, Kim DB, et al. Neuroprotective effect of green tea extract in experimental ischemia-reperfusion brain injury. Brain Res Bull 2000;53(6):743–9.
37 Lührs T, Ritter C, Adrian M, Riek-Loher D, Bohrmann B, Döbeli H, et al. 3D structure of Alzheimer's amyloid-β (1–42) fibrils. Proc Natl Acad Sci U S A 2005;102(48):17342–7.
38 Nelson R, Sawaya MR, Balbirnie M, Madsen AØ, Riekel C, Grothe R, et al. Structure of the cross-β spine of amyloid-like fibrils. Nature 2005;435(7043):773–8.
39 Ono K, Yoshiike Y, Takashima A, Hasegawa K, Naiki H, Yamada M. Potent anti-amyloidogenic and fibril-destabilizing effects of polyphenols in vitro: implications for the prevention and therapeutics of Alzheimer's disease. J Neurochem 2003;87(1):172–81.
40 Reinke AA, Gestwicki JE. Structure–activity relationships of amyloid beta-aggregation inhibitors based on curcumin: influence of linker length and flexibility. Chem Biol Drug Des 2007;70(3):206–15.
41 Katayama S, Ogawa H, Nakamura S. Apricot carotenoids possess potent anti-amyloidogenic activity in vitro. J Agric Food Chem 2011;59(23):12691–6.
42 Ehrnhoefer DE, Bieschke J, Boeddrich A, Herbst M, Masino L, Lurz R, et al. EGCG redirects amyloidogenic polypeptides into unstructured, off-pathway oligomers. Nat Struct Mol Biol 2008;15(6):558–66.
43 Hudson SA, Ecroyd H, Dehle FC, Musgrave IF, Carver JA. (-)-Epigallocatechin-3-gallate (EGCG) maintains κ-casein in its pre-fibrillar state without redirecting its aggregation pathway. J Mol Biol 2009;392(3):689–700.
44 Bendary E, Francis R, Ali H, Sarwat M, El Hady S. Antioxidant and structure–activity relationships (SARs) of some phenolic and anilines compounds. Ann Agric Sci 2013;58(2):173–81.